



# The Effect of Demand-Response Program and Distributed Generation Resources on Optimal Establishment of Electric Vehicle Charging/Discharging Stations Using a Triple Optimization Algorithm

Monireh Ahmadi<sup>1</sup>, Seyed Hossein Hosseini <sup>\*1,2</sup>, Murteza Farsadi <sup>1,3</sup>

<sup>1</sup>Department of Electrical Engineering, Urmia Branch, Islamic Azad University, Urmia, Iran, monir.ahmadi@gmail.com

<sup>2</sup>The Engineering Faculty, Near East University, 99138Nicosia, North Cyprus, Mersin 10, Turkey, hossein.medi@vatanmail.ir

<sup>3</sup>Istanbul Aydin University ,Engineering Faculty , Department of Electrical and Electronics Engineering, Istanbul,Turkey, m.farsadi@urmia.ac.ir

## Abstract

This study investigated the effect of distributed generation resources and demand-response program on the placement of charging/discharging stations and optimal exploitation programming of electric vehicles in a distribution network. Effective factors in the sitting of stations and optimal charge/discharge power in stations are a combination of technical and economic parameters. Minimization of network losses, minimization of voltage loss in feeders, smoothing network load curve, and THD reduction were assumed as technical parameters. As to the economic scope, the placement of stations and charge/discharge power were considered the most effective parameters. In other words, the costs of charging/discharging operations needed to be minimized in the stations to reach the lowest costs spent on purchasing power. A price-based demand-response program was incorporated into the simulations to manage loads on the customer side and smooth the load curve. We implemented genetic, particle swarm optimization, and imperialist competitive hybrid meta-heuristic algorithms to find the optimum operating point. We performed simulations in an IEEE standard 69-bus network. The problem was solved using the former hybrid algorithm, and optimal sites of stations and exploitation program of charge/discharge were specified. This study evaluated the effects of renewable energy resources and price-based demand-response program on the optimal placement of stations and optimal exploitation program of stations. Furthermore, it addressed the effects of an increase in the number of stations and a rise in charge/discharge capacity.

*Keywords:* Optimal placement. electric vehicles. hybrid meta-heuristic algorithms. charging/discharging stations. demand-response program. distributed generation resources

Article history: Received 29-Mar-2021; Revised 03-Apr-2021; Accepted 21-May-2021. Article Type: Research Paper

© 2021 IAUCTB-IJSEE Science. All rights reserved

<http://dx.doi.org/10.30495/ijsee.2021.681964>

## 1. Introduction

Nowadays, the optimal sitting of charging / discharging stations and charging/discharging processes in different hours is highly incorporated into exploitation programs of electric vehicles in electric networks. One of the factors affecting the optimal placement of stations and exploitation programming is the demand-response program and load management on the customer side (Sabzehgar et al. 2020). Some designs included distributed generation resources and renewable energy resources for the optimal placement of charging stations (Jiang et al. 2017; Domínguez-Navarro et al. 2019; Mouli et al. 2016; Tabatabaee et al. 2017;

Hafez and Bhattacharya 2017). Furthermore, researchers determined the capacity of distributed generation resources and locations of electric vehicle charging stations by different optimized methods (Mirzaei et al. 2016; ISLAM et al. 2016). (Mendes et al. 2016; Luo et al. 2020) designed electric vehicle charging systems inside microgrid, and controlled vehicle-to-grid (V2G) interaction.

The present study aims to obtain the optimal locations of electric vehicle charging stations in the network, considering distributed generation resources. The available stations have both charging and discharging capabilities, and defines the

objective function as a set of financial and technical parameters.

## 2. Problem description

Relation (1) defines the main objective function of this study by relation (1) regarding all of the concerned parameters. Relation (1) includes technical and financial items.

$$\text{Objective Function} = \min[(W_1 \times f_1 + W_2 \times f_2 + W_3 \times f_3 + W_4 \times f_4) + W_5 \times f_5] \quad (1)$$

Where  $W_1, W_2, W_3, W_4,$  and  $W_5$  are weighting coefficients.  $f_1$  stands for the total losses in the network over 24 hours, as given below:

$$f_1 = \sum_{t=1}^{24} \sum_{i=1}^{\text{line number}} R_{\text{line}_i} |I_{\text{line}_i,t}|^2 \quad (2)$$

Where  $I_{\text{line}_i}$  represents the passing current of the  $i^{\text{th}}$  line at the  $t^{\text{th}}$  hour and  $R_{\text{line}_i}$  denotes the resistance of the  $i^{\text{th}}$  line. Also,  $f_2$  represents the total voltage losses in the network over 24 hours (after incorporation of renewable energy resources), which is defined by relation (3).

$$f_2 = \sum_{t=1}^{24} \sum_{i=1}^{\text{bus number}} |1 - V_{i,t}| \quad (3)$$

Where  $V_{i,t}$  denotes the voltage at the  $i^{\text{th}}$  bus at the  $t^{\text{th}}$  hour. Further,  $f_3$  is the energy consumption cost function, which comprises three main parts, as defined in what follows. The cost of consumption in the network that needs to be paid to the distribution company. In this regard, first, the total receiving power from the substation must be calculated. According to the renewable energy resources and electric vehicles in the network, we calculated the input power provided by the substation at the  $t^{\text{th}}$  hour as follows:

$$P_{\text{sub},t} = \sum_{i=1}^{N_{\text{bus}}} P_{d,i,t} + \sum_{j=1}^{N_{\text{line}}} P_{\text{loss},j,t} - \sum_{k=1}^{N_{\text{station}}} P_{\text{disch},k,t} + \sum_{k=1}^{N_{\text{station}}} P_{\text{ch},k,t} - P_{\text{wind},t} - P_{\text{pv},t} \quad (4)$$

Where:

$P_{\text{sub},t}$ : Input power provided by the substation at the  $t^{\text{th}}$  hour (kW)

$P_{d,i,t}$ : Demand active power at the  $i^{\text{th}}$  bus and  $t^{\text{th}}$  hour (kW)

$P_{\text{loss},j,t}$ : Power losses in the  $j^{\text{th}}$  line at the  $t^{\text{th}}$  hour (kW)

$P_{\text{disch},k,t}$ : Discharged power from electric vehicles to the network at the  $k^{\text{th}}$  station and  $t^{\text{th}}$  hour (kW)

$P_{\text{ch},k,t}$ : Charged power from the network to electric vehicles at the  $k^{\text{th}}$  station and  $t^{\text{th}}$  hour (kW)

$P_{\text{wind},t}$ : Generated power in the wind section of the renewable energy production unit at  $t^{\text{th}}$  hour (kW)

$P_{\text{pv},t}$ : Generated power in the solar section of the renewable energy production unit at  $t^{\text{th}}$  hour (kW)

$N_{\text{bus}}, N_{\text{line}},$  and  $N_{\text{station}}$  are the number of busses, line, and electric vehicle charging/discharging stations in the network, respectively.

Given the input power calculated by relation (4), the cost to be paid to the distribution company is calculated by relation (5), assuming that the distribution company takes a 20% profit.

$$f_6 = \sum_{t=1}^{24} 1.2 * P_{\text{sub},t} * C_t \quad (5)$$

Where  $C_t$  represents the cost of purchased energy by the distribution company at the  $t^{\text{th}}$  hour from the network power plant units. Table 1 lists the energy price per hour (\$/hour), considering three temporal periods (off-peak, average, and peak hours). The electric vehicle charge/discharge costs at the stations include two other parts due to the presence of electric vehicles in the network.

- The cost to be received from vehicle owners during the charging process at the stations
- The cost to be paid to vehicle owners once discharging vehicle batteries to the network

The sum of these costs is calculated by relation (6). As can be observed in this relation, to encourage customers (vehicle owners), the discharge cost paid to them is 10% higher than the charge cost that the main network receives, which could be a tempting profit at peak hours.

$$f_7 = \sum_{t=1}^{24} (C_t * \sum_{k=1}^{N_{\text{station}}} P_{\text{ch},k,t} - 1.1 * C_t * \sum_{k=1}^{N_{\text{station}}} P_{\text{disch},k,t}) \quad (6)$$

Table 1 lists the profit and cost of electric vehicles for the customers. As can be seen in Table 1, vehicle owners can purchase electrical energy during off-peak and average hours (when the energy price is lower) and sell it during peak hours (when the energy price is higher).

Table.1.  
Calculation of the profit offered to electric vehicle owners

Period	Off-peak	Average	Peak
Hour	[23-9]	[10-18]	[19-23]
Power price per kW.h (\$)	10	15	20
Price of power purchased by vehicle owners from distribution company per kW.h (\$)	12	18	24
Price of power sold by vehicle owners to distribution company per kW.h (\$)	11	16.5	22

In relation (1),  $f_3$  represents the cost function and is defined as follows:

$$f_3 = f_6 + f_7 \quad (7)$$

Since the parameters used in the objective function (including cost, power loss, and voltage loss) are not of the same type, the objective function needs to be corrected by pre-uniting these quantities relative to the initial state, when there is no electric vehicle charging station.

Moreover,  $f_4$  stands for the total harmonic distortions of current and voltage over 24 hours of a day at charging station and  $W_4$  is the weighting coefficient considered for distortion. Thus,  $f_4$  is calculated as follows:

$$f_4 = \sum_{t=1}^{24} \sum_{i=1}^{bus\ number} (TDD_{i,t} + THD_{i,t}) \quad (8)$$

Where  $TDD_{i,t}$  and  $THD_{i,t}$  represent the harmonic distortions of current load and voltage, respectively, at the  $i^{\text{th}}$  bus and  $t^{\text{th}}$  hour of the day.  $TDD_{i,t}$  And  $THD_{i,t}$  are calculated by relations (9) and (10), respectively.

$$TDD_{i,t} = \left(\frac{8}{1500}\right) * CH_{i,t} \quad (9)$$

$$THD_{i,t} = \left(\frac{5}{1500}\right) * CH_{i,t} \quad (10)$$

Similar to other parameters available in the objective function,  $f_5$  was pre-united relative to its maximum value feasible in simulations. The maximum values of  $f_5$  occurs at the highest possible power of electric vehicle charging (1.5 MW for each station), at both stations during 24 hours of the day. In this paper, we assumed the charging power at the stations as entirely standard. IEEE519-1992 is one of the standards that has addressed the harmonic distortion induced by electric vehicle charging. Relations (9) and (10) have been presented in the IEEE519-1992 standard regarding the reasonable maximum values of THD and TDD. Also, a direct relationship has been assumed between the electric vehicle charged/discharged power and harmonic distortion.

Moreover,  $f_5$  indicates the effects of constraints imposed by electric vehicle performance. If the problem constraints are resolved,  $f_5$  takes a zero-value. Generally,  $f_5$  is calculated by relation (11).

$$f_5 = n * k_{er} \quad (11)$$

Where  $n$  is the number of unsatisfied constraints and  $k_{er}$  is a constant value that is usually considered higher than the values of main parts of the objective function.  $f_4$  was defined to be able to solve the problem by meta-heuristic algorithms and incorporation of constraints into the objective function. The constraints imposed on the problem are as follows:

### 3. Charge/discharge power

The charge/discharge power at any station must always be lower than the capacity of the station at any time.

$$0 \leq CH_{i,t} \leq Cap_i \quad i = 1:n \quad (12)$$

$$0 \leq DisCH_{i,t} \leq Cap_i \quad i = 1:n$$

Where  $CH_{i,t}$  and  $DisCH_{i,t}$  denote the charge and discharge values at the  $i^{\text{th}}$  station and  $t^{\text{th}}$  hour, respectively.  $Cap_i$  Represents the capacity of the  $i^{\text{th}}$  station, and  $n$  is the number of charging and discharging stations.

#### A) Sum of charge and discharge power

Several charging and discharging devices are used at any station that some of them might be charging, and some others might be discharging electric vehicles during each hour. The total exchanged electric power in these devices is not allowed to exceed the total capacity of the station. The sum of charge and discharge power needs to be lower than the station's capacity (relation (13)).

$$0 \leq CH1_{i,t} + DisCH1_{i,t} \leq Cap_i \quad i = 1:n \quad (13)$$

#### B) Prediction of the electric power exchange between the network and electric vehicles

The total power charged to electric vehicles (from the network) minus the total discharged power from the network (to electric vehicles) need to equate to the predicted power. The following relation expresses this constraint:

$$\sum_{i=1}^n P_{Ch\ i,t} - \sum_{i=1}^n P_{Disch\ i,t} = P_{predic,t} \quad (14)$$

Where  $P_{predic,t}$  is the predicted consumed-power for the set of electric vehicles at the  $t^{\text{th}}$  hour.

#### C) Implementation of the demand-response program

In the model of the price-based demand-response program proposed in this paper, load shift and load interruption can simultaneously occur. Also, the behavior of customers can be optimized by pricing consumption periods and transferring demand from peak to off-peak hours. The effect of the price-based demand-response program on customer satisfaction can be defined by the elasticity coefficient as follows:

$$e_{st} = \frac{\Delta L_s / L_s^0}{\Delta P_t / P_t^0} \begin{cases} e_{st} \leq 0, & \text{if } s = t \\ e_{st} \geq 0, & \text{if } s \neq t \end{cases} \quad (15)$$

Where  $s$  stands for time ( $s=1,2,3, \dots, T$ ) and other parameters are defined as follows:

$\Delta L_s$  : Variations in consumed load after implementing the price-based demand-response program

$L_s^0$  : Consumed load before the price-based demand-response program

$\Delta P_t$  : Variations in electricity price after implementing the price-based demand-response program

$P_t^0$  : Electricity price before the price-based demand-response program.

If the electricity price varies in different periods, the customer response can be expressed in two forms. As the first response, a customer can activate those loads that cannot be transferred to other periods (i.e., lighting loads). Such loads that are sensitive only to one period are called self-elasticity, whose elasticity coefficient is always negative. In the second response, some loads can be transferred from the peak period to off-peak periods. Such behavior is called multi-stage elasticity and is evaluated by the cross-elasticity coefficient, which is always positive. The mathematical description of the problem is offered in detail in what follows.

- When  $s = t$ ,  $e_{st}$  is called self-elasticity. Only load interruption can occur and  $e_{st}$  is always negative.
- When  $s \neq t$ ,  $e_{st}$  is called cross-elasticity. In this mode, the load shift can occur,  $e_{st}$  is always positive, and load variations will be positive as well.

We calculated Load variations ( $L_t$ ) after implementing the price-based demand-response program by relation (16).

$$L_t = L_t^0 \times \left\{ 1 + e_{tt} \times \frac{[P_t - P_t^0]}{P_t^0} + \sum_{s \neq t}^{24} e_{st} \times \frac{[P_s - P_s^0]}{P_s^0} \right\} \quad (16)$$

The profit made by selling electricity varies using the price-based demand-response program. The difference in profits made by selling electricity before and after implementing the time-dependent load response program ( $\pi_t^{PB}$ ) is calculated by relation (17).

$$\pi_t^{PB} = P_t^0 L_t^0 - (P_t^0 + \Delta P_t) L_t \quad (17)$$

In the demand-response program, the coefficient of load elasticity to temporal price variations plays a key role in the calculations. This coefficient that is attributed to the reaction of customers to price change depends on some important parameters, including social, cultural, and economic behavior. The elasticity coefficient in the present paper was obtained from Ref. (Sabzehgar et al. 2020). Since one can divide the consumption in a 24-hour cycle into three periods, i.e., off-peak,

average, and peak, we took 9 states into account for the elasticity coefficient (Table 2).

Table.2.  
The coefficient of load elasticity to temporal price variations during different periods

	<i>Off-peak hours</i>	<i>Average hours</i>	<i>Peak hours</i>
Off-peak hours	-0.2	0.008	0.006
Average hours	0.01	-0.2	0.008
Off-peak hours	0.012	0.016	-0.2

The maximum allowable load variations in the demand-response program must be limited to avoid excessive load transfer to off-peak hours since it would cause a new peak period. In the present study, the maximum allowable load variations in the demand-response program were limited to 10% of the predicted initial load. In other words, loads are permitted to increase or decrease by 10% during different hours of the day.

#### 4. Problem-solving in the sample test network

We selected the standard 69-puls IEEE network as the test network in the present study. Also, we used the genetic, particle swarm optimization (PSO), and imperialist competitive meta-heuristic algorithms to solve the problem mentioned above. In this regard, we solved the problem first by the genetic algorithm, and the obtained results were then used as the input data for the PSO and imperialist competitive algorithms. The problem variables included the possibility of establishing charging/discharging stations and charging/discharging status at the stations. Two renewable energy resources were assumed to be available at buses 61 and 63. In addition, the total consumed power by the set of electric vehicles in the network was definite at each moment and included in the problem data. We disregarded the uncertainty of renewable energy resources, and the profile of electric power generation by wind and solar resources was assumed as shown in Fig. 1. Each renewable unit included both wind and solar resources. We set the maximum possible power in the entire wind and solar resources at 1MW (solar and wind resources with the maximum power of 0.5 MW each). The renewable energy resources were located using the genetic algorithm to minimize power and voltage losses in the network.

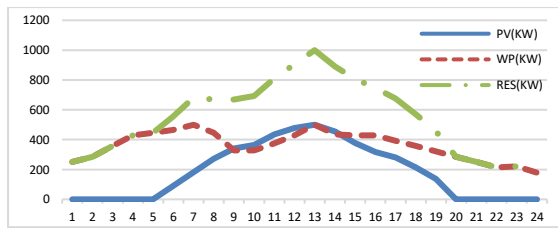


Fig. 1. Generation power in the renewable energy resource (kW) at different times of the day

In the concerned test network, we assumed two electric vehicle charging stations with a capacity of 1.5MW. Fig. 2 indicates the total consumed load by electric vehicles. In this figure, the negative amount of consumed power by electric vehicles implies that they are injecting active power to the network. Similarly, a positive amount of consumed power by electric vehicles indicates that they are receiving energy from the network. In the 69-bus network, the active power consumption (during 24 hours) is 73MW when there is no renewable energy resource and electric vehicle, and the demand-response program is not implemented. When we consider two renewable energy resources, the demand power supplied by the network decreases to 47MW. In this study, given the base load of 47MW (during 24 hours), electric vehicles were used such that the minimum frequency fluctuations and the smoothest load curve were reached. In other words, we programed the behavior of electric vehicles regarding the minimization of frequency deviation and the smoothing process of the load curve.

In this paper, we carried out the optimal placement of charging/discharging stations and optimal electric vehicle programming by genetic, PSO, and imperialist competitive meta-heuristic algorithms. We divided the problem's objective function into three main parts; then optimized each part by one of the former algorithms. The optimization process was performed first by the genetic algorithm, then PSO algorithm, and the imperialist competitive algorithm in the end. We used the obtained results in each section as the input data to the next section.

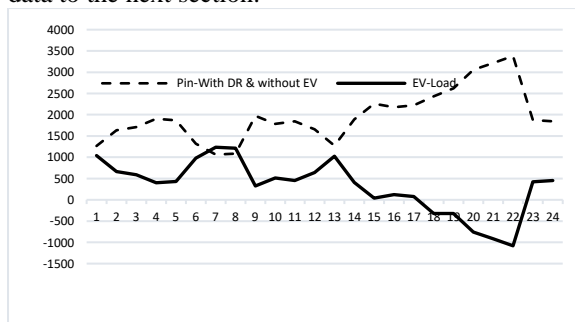


Fig. 2. Electric vehicle consumption and other loads in the standard 69-bus IEEE network

## 5. Problem-solving

In the simulations of this study, we implemented the binary genetic algorithm and used the PSO algorithm was used in the binary state as well. Six scenarios were defined to investigate the effect of the demand-response program and distributed resources.

A: Absence of distributed resources; without the implementation of the demand-response program

B: Absence of distributed resources; with the implementation of the demand-response program

C: Presence of distributed resources; without the implementation of the demand-response program

D: Presence of distributed resources; with the implementation of the demand-response program

E: Increase in the number of stations

F: Increase in the capacity of devices

Figs. 3-10 present the results obtained during the simulations of the last part of the triple algorithm for six scenarios. Since the imperialist competitive part included all of the parameters of the objective function, the figures show the simulation results for the imperialist competitive section. In the scenario F, the number of stations increased from 2 to 4 and the charging/discharging capacity of stations was raised from 1.5 to 1.8MW in the scenario E. Fig. 3 shows the objective function in the six scenarios. As can be observed, the objective function offered a descending trend in all scenarios, and its size was reduced as the algorithm approached the optimal point. Also, when we did not incorporate the distributed resources into the simulations, the size of the objective function substantially increased compared to other modes. The objective function took the minimum optimal value In scenario D. Figs. 4 and 5 depict the charge/discharge cost curves during the imperialist competitive algorithm. As can be observed, In scenario B, electric vehicle charge/discharge costs were dramatically lower than that of other states. On the contrary, In scenario D, electric vehicle charge/discharge costs increased. The decrease in charge/discharge costs might be due to the decrease in the amount of charge and discharge, particularly during peak hours. In other words, by implementing the demand-response program, loads were transferred from the peak to off-peak hours (i.e., smoothing of load curves). Therefore, electric vehicle owners would have fewer customers during peak hours and, in turn, the amount of electric vehicle charge/discharge would decrease, leading to lower charge/discharge costs. Under the available conditions of the concerned network, as the load curve becomes more smoothed and price difference becomes higher between different hours, vehicle owners would be directed to

the power trade in the network, attempt to buy power in off-peak hours, store it, and sell it in peak-hours to make a higher profit. The demand-response program prevents load accumulation in peak hours and, thus, the demand is reduced in peak hours. Therefore, electric vehicles have lower participation in the network (lower energy exchange). In scenario D, a great portion of the power generated by renewable resources was injected into the network, which could be purchased by vehicle owners in off-peak hours and sold in peak hours. Hence, charge and discharge costs significantly increased compared to other states. In scenario D, charge and discharge costs were at the middle level (compared to the scenarios B and C) so that the increase in the number of stations and charge/discharge capacity changed charge and discharge costs negligibly.

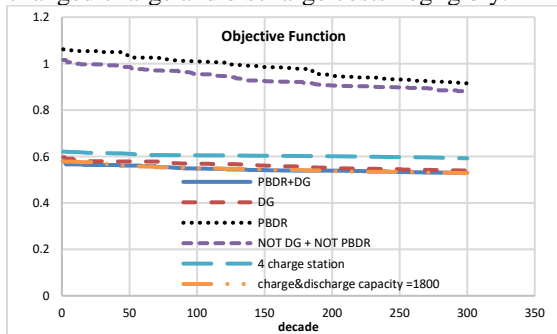


Fig. 3. Objective function in the imperialist competitive part of the triple algorithm

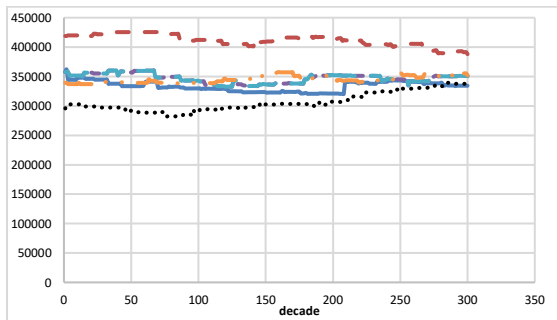


Fig. 4. Electric vehicle charge cost in the imperialist competitive part of the triple algorithm

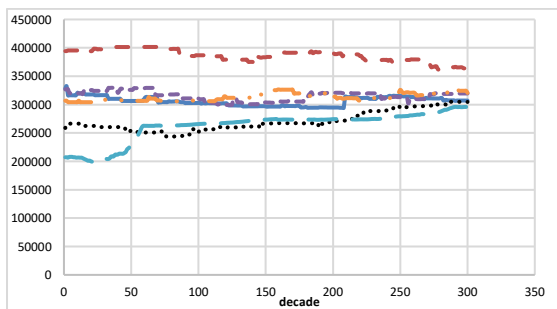


Fig. 5. Electric vehicle discharge cost in the imperialist competitive part of the triple algorithm

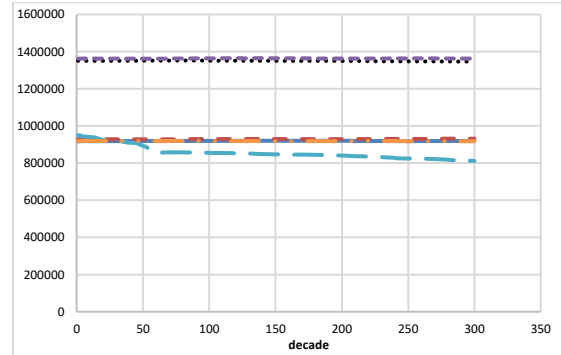


Fig. 6. Total cot in the imperialist competitive part of the triple algorithm

Fig. 6 illustrates the total cost in the imperialist competitive part of the triple algorithm. As can be observed, when distributed generation resources were not available in the network, the total cost was considerably lower than that of other states, and the implementation of the demand-response program had an insignificant effect on the total cost. In other words, in the absence of distributed generation resources, the required power must be purchased from the distribution company and, thus, the total cost was escalated. Furthermore, the increase in the number of stations led to a decrease in costs as well. According to Figs. 4 and 5 and regarding the ultimate optimal response, when there were four stations, the charge cost was higher than the discharge cost; therefore, the profit earned by vehicle owners was reduced, i.e., lower total cost. Fig. 7 presents the voltage loss in the imperialist competitive part of the triple algorithm. As can be seen, the absence of distributed generation resources caused a rise in the voltage loss in the network, whereas the implementation of the demand-response program degraded the conditions. In scenario C, the minimum voltage loss was obtained. In scenario D, the increase in the number of charging and discharging stations resulted in the elevations of voltage loss in the network; however, the increase in the capacity of stations negligibly affected the voltage loss in this state.

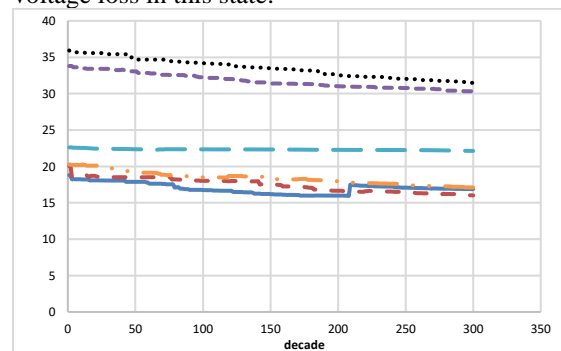


Fig. 7. Voltage loss in the imperialist competitive part of the triple algorithm

Fig. 8 shows the power losses in the imperialist competitive part of the triple algorithm. As can be seen, similar to the results of voltage loss, the absence of distributed generation resources led to an increase in the power losses in the network, while the implementation of the demand-response program degraded the conditions (i.e., increasing power losses). In scenario D, the minimum power losses were obtained in the network. In scenario D, the increase in the capacity of charging and discharging stations reduced power losses in the network; however, the increase in the number of stations augmented power losses. Figure 9 shows the input power to the network in the imperialist competitive part of the triple algorithm. As can be observed in this figure, for scenarios with no distributed resources, the input power to the network (purchased power from the distribution company) was markedly higher than that of the scenarios with distributed resources.

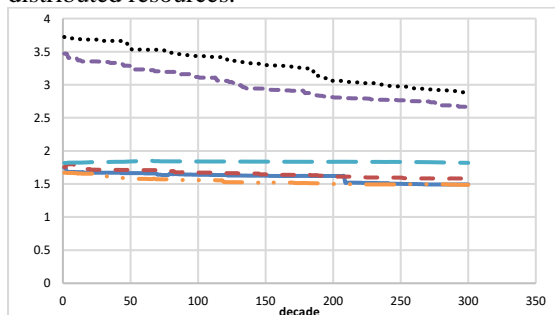


Fig. 8. Power losses in the imperialist competitive part of the triple algorithm

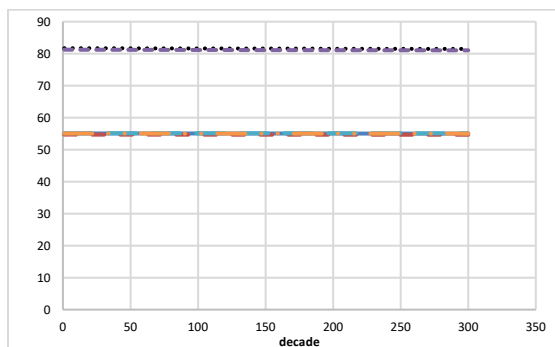


Fig. 9. Input power in the imperialist competitive part of the triple algorithm

Fig. 10 depicts the harmonic distortions induced by exploiting charging and discharging stations in the imperialist competitive part of the triple algorithm for all of the six scenarios. In scenario A, the energy exchange between the network and electric vehicles was raised. Thus, the harmonic distortions induced by vehicles were elevated, which can be validated by the consistency between Figs. 4, 5, and 9. The implementation of the demand-response program led to a decrease in the harmonic distortions in the network, and the increase in both the number and capacity of stations

further reduced harmonic distortions triggered by the operations of electric vehicles in the stations. It is worth noting the increase in the number of stations was more effective than the increase in their capacity in reducing harmonic distortions.

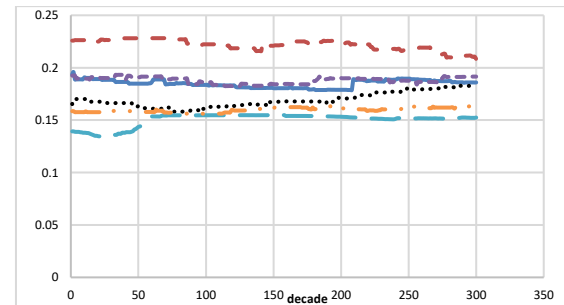


Fig. 10. Harmonic distortions in the imperialist competitive part of the triple algorithm

Table 3 lists the ultimate optimal responses for the six scenarios obtained by the algorithm. This table also presents the optimal locations predicted by the algorithm to establish charging and discharging stations in each scenario. As can be observed, busses 4 and 61 are the optimal locations to found charging and discharging stations In scenario D. Moreover, the absence of the demand-response program and distributed generation resources along with the increase in the capacity of charging and discharging stations have posed no effect on the optimal placement of charging and discharging stations. Also, as the number of stations increased from 2 to 4, the algorithm suggested neither of the previously predicted locations, but it introduced discretely different locations as the optimal sites of stations.

Figs. 11-14 show the ultimate optimal response for the 24-hour charging/discharging programming at the two stations. As can be observed, the demand-response program had a significant effect on the optimal charging /discharging pattern at the stations. In scenario D, the triple algorithm offered an entirely different pattern for the optimal charging/discharging program at the stations. However, in the three other scenarios (scenarios A, B, and C), identical behavior can be observed at the stations in terms of optimal charge/discharge power. Based on the obtained results, various states of optimal charging/discharging program can be met at the stations to reduce costs and optimize qualitative/quantitative parameters.

## 6. Conclusions

This study has proposed an initial pattern for total charge and discharge power in the network. We have set the total charge and discharge power so that the absorbed power in the entire network would be uniform. However, before the charging/discharging program, we used the distributed generation

resources and implemented the demand-response program as well. The use of distributed generation resources has led to a decrease in the input power to the network and allowed reaching the paper objectives, namely reduction of power losses, voltage loss, and exploitation costs. Then, considering charging stations in several points of the network, we determined the optimal location of stations and charge/discharge power in each station per hour to reduce the power losses of the network, voltage loss, and costs paid to purchase the network's total consumption power. This problem was addressed in a standard 69-bus IEEE network. We implemented three meta-heuristic algorithms to solve the problem, including genetic, PSO, and imperialist competitive. First, we solved the problem with the genetic algorithm concerning all components of the objective function. Then, we solved the problem by the genetic algorithm by considering a part of the objective function and used the obtained results as the input data to the PSO and imperialist competitive algorithms. In other words, in addition to the genetic algorithm, the problem was solved by triple algorithms.

Table.3.  
Comparison of the obtained results in different scenarios using the triple algorithm

	Charge & Discharge Capacity =1800K W	4Charge & Discharge Station	Not DG + Not PBDR	PBDR	DG	PBDR +DG
Optimal Location	61,4	6, 30, 39,45	61, 28	61,4	61, 4	61,3
Charge cost (\$)	334357	388000	337480	350985	216458	351950
Discharge cost (\$)	307099	360257	304685	319540	296856	320602
Total cost	919160	931791	1346724	1362836	811419	917932
Total input power (MW)	55.0212	54.658	81.484	81.041	55.107	55.020
Power losses (Pu)	1.493	1.583	2.881	2.666	1.819	1.487
Voltage loss (Pu)	16.877	16.009	31.483	30.312	22.120	17.109
THD (Pu)	0.18591	0.2081	0.182	0.192	0.152	0.162

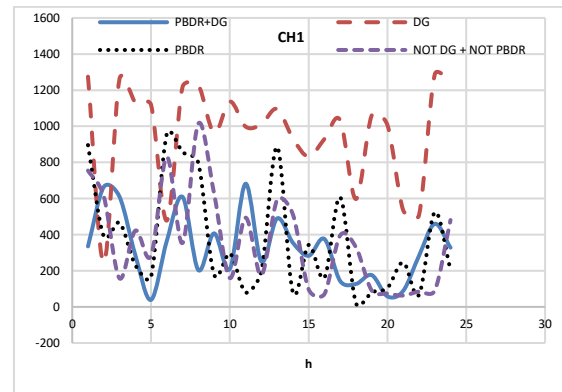


Fig. 11. Ultimate optimal response as to the charging process at station No. 1 in different scenarios

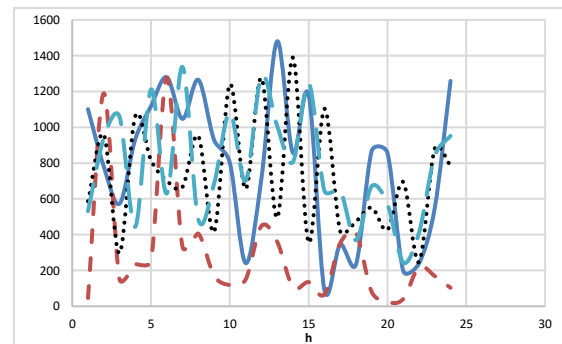


Fig. 12. Ultimate optimal response as to the charging process at station No. 2 in different scenarios

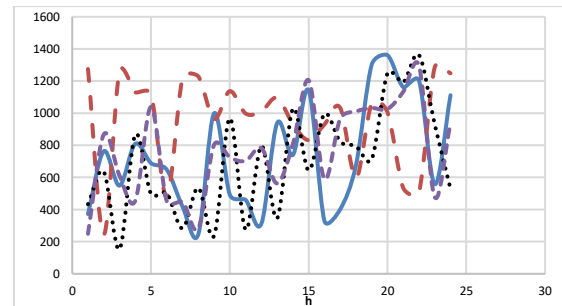


Fig. 13. Ultimate optimal response as to the discharging process at station No. 1 in different scenarios

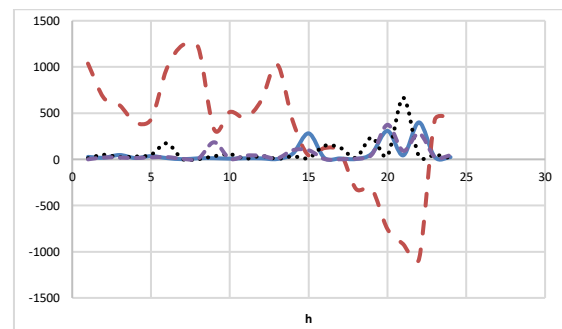


Fig. 14. Ultimate optimal response as to the discharging process at station No. 2 in different scenarios

The obtained results by the three algorithms have revealed almost the same charge and discharge at the stations and suggested identical sites to

establish the stations. The genetic-imperialist competitive algorithm outperformed the other two algorithms, with better power losses and voltage loss. Previous studies have used various parameters in the objective function to determine the optimal locations of electric vehicle charging stations, and their electric systems might differ from the 69-bus system proposed in this paper. Hence, it was difficult to compare the results of this study with the findings of previous studies. For instance, Ref. (Moradi et al. 2015) carried out the simultaneous siting of distributed generation resources and charging stations, and suggested buses 61 and 22 as the proper locations to establish charging stations. The curve of total charge and discharge of electric vehicles presented in Re. (Moradi et al. 2015) is different from that of the present paper. Therefore, the suggested site for the establishment of sites is different from the results obtained by the present study. In this study, we have considered the curve of total charge and discharge of electric vehicles so that the network load curve would be smooth. It is worth noting that this is the first study on the optimal charging/discharging programming at the electric vehicle charging/discharging stations using genetic, PSO, and imperialist competitive algorithms in hybrid modes, whereas previous studies implemented one algorithm or at most two evolutionary algorithms to solve the problem of optimal siting of charging/discharging stations.

## References

- [1]. JA. Domínguez-Navarro, Dufo-López R, Yusta-Loyo JM, Artal-Sevil JS, Bernal-Agustín JL (2019) Design of an electric vehicle fast-charging station with integration of renewable energy and storage systems. *International Journal of Electrical Power & Energy Systems*. 105, 46-58.
- [2]. O. Hafez, K. Bhattacharya (2017) Optimal design of electric vehicle charging stations considering various energy resources. *Renewable energy*, 107, 576-589.
- [3]. M. ISLAM, H. Shareef, A. Mohamed (2016) Optimal siting and sizing of rapid charging station for electric vehicles considering Bangi city road network in Malaysia. *Turkish Journal of Electrical Engineering & Computer Sciences*, 24(5), 3933-48.
- [4]. X. Jiang, J. Wang, Y. Han, Q. Zhao (2017) Coordination dispatch of electric vehicles charging/discharging and renewable energy resources power in microgrid. *Procedia Computer Science*, 107(4), 157-163.
- [5]. L. Luo, Z. Wu, W. Gu, H. Huang, S. Gao, J. Han (2020) Coordinated allocation of distributed generation resources and electric vehicle charging stations in distribution systems with vehicle-to-grid interaction. *Energy*, 192, p.116631.
- [6]. PR. Mendes, LV. Isorna, C. Bordons, JE. Normey-Rico (2016) Energy management of an experimental microgrid coupled to a V2G system. *Journal of Power Sources*, 327, 702-713.
- [7]. MJ. Mirzaei, A. Kazemi, O. Homaei (2015) A probabilistic approach to determine optimal capacity and location of electric vehicles parking lots in distribution networks. *IEEE Transactions on industrial informatics*, 12(5), 1963-1972.
- [8]. MH. Moradi, M. Abedini, SR. Tousei, SM. Hosseini (2015) Optimal siting and sizing of renewable energy sources and charging stations simultaneously based on Differential Evolution algorithm. *International Journal of Electrical Power & Energy Systems*, 73, 1015-1024.
- [9]. GC. Mouli, P. Bauer, M. Zeman (2016) System design for a solar powered electric vehicle charging station for workplaces. *Applied Energy*, 168, 434-443.
- [10]. M. Rahmani-andebili (2016) Modeling nonlinear incentive-based and price-based demand response programs and implementing on real power markets. *Electric Power Systems Research*, 132, 115-124.
- [11]. R. Sabzehgar, MA. Kazemi, M. Rasouli, P. Fajri (2020) Cost optimization and reliability assessment of a microgrid with large-scale plug-in electric vehicles participating in demand response programs. *International Journal of Green Energy*, 17(2), 127-136.
- [12]. S. Tabatabaee, SS. Mortazavi, T. Niknam (2017) Stochastic scheduling of local distribution systems considering high penetration of plug-in electric vehicles and renewable energy sources. *Energy*, 121, 480